Available online at www.cuijca.com

INTERNATIONAL JOURNAL OF COMPUTATIONAL ANALYSIS

Vol (5), No. (1), pp. 31-46

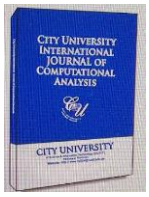

Dynamics and Transmission of COVID-19 Epidemic in Malaysia: Atangana-Baleanu Fractional Model

Muhammad Arif1[2*], Poom Kumam[1,2,3], Zubair Ahmad[4], and Amir Khan[5]

[1]*Fixed Point Research Laboratory, Fixed Point Theory and Applications Research Group, Center of Excellence in Theoretical and Computational Science (TaCS-CoE), Faculty of Science, King Mongkut's University of Technology Thonburi (KMUTT), 126 Pracha Uthit Rd., Bang Mod, Thung Khru, Bangkok 10140, Thailand*

[2]*Center of Excellence in Theoretical and Computational Science (TaCS-CoE), Faculty of Science, King Mongkut's University of Technology Thonburi (KMUTT), 126 Pracha Uthit Rd., Bang Mod, Thung Khru, Bangkok 10140, Thailand*

[3]*Department of Medical Research, China Medical University Hospital, China Medical University, Taichung 40402, Taiwan*

[4]*Dipartimento di Matematica e Fisica, Università degli Studi della Campania ''Luigi Vanvitelli'', 81100 Caserta, Italy*

[5]*Department of Mathematics, University of Swat, KPK, Pakistan*

**Corresponding author: Muhammad Arif:*

Keywords:
COVID-19; SEIR fractional model for Malaysia; stability analysis.

A B S T R A C T

The purpose of this article is to specify the passage and mathematical model of COVID-19. The infectious disease COVID-19 originated in China and has affected the whole world. In the present study, we have considered, the SEIR model to evaluate the spread of COVID-19 in Malaysia. In this article, we have explored the gesture of COVID-19 accurately by applying the newly advanced fractional operator of Atangana-Baleanu to the classical SEIR model. Based on (WHO) reported data in this study, we discussed the corona's virus's behaviour in Malaysia. We have taken the available infection cases from 1st May 2020 to 14th May 2020. We have matched our problem to Malaysia's actual data, which shows a firm agreement with the actual data. Based on data gathered by the World Health Organization (WHO), we have determined the basic reproduction number for the studied disease. Furthermore, we conducted a stability analysis for both the Disease Free Equilibrium (DFE) and the Endemic Equilibrium (EE) in order to understand the behavior of the model in terms of disease spread and persistence. The fractional model provided was solved through numerical methods using MATLAB software. We visually depicted and extensively discussed the impact of various parameters. Notably, our study projected the disease progression for the next 300 days through an approximation.

1. Introduction

There are many infectious diseases that affect humans as well as animals. HIV, hepatitis B and C, avian flu, malaria, Ebola virus, dengue virus, tuberculosis, chickenpox, diarrhoea, influenza, rubella illness, Pine wilt, Moko, orange rust, Karnal bunt, Dutchelm, and sugar cane, among others, are among the infectious diseases. [1]. It is imperative to study these infectious diseases and to find possible strategies to control them. During the study of these infectious diseases, one can see how these infections spread, and attention to the desirable feasible assets to identify these diseases to hamper them from spreading.

Recently, an infectious disease has been observed, namely, the novel Coronavirus (COVID-19). The initial case of the novel coronavirus in a human was identified on 31st December 2019, in Wuhan, China. The Covid-19 symptoms were initially misdiagnosed as pneumonia. The infected individual did not recover after vaccination and pneumonia medication, and the medication was ineffective [2]. Experts then clarified that this isn't pneumonia. Second, it was discovered that the virus propagated quickly from humans to people in China. Moreover, the contaminated cases were not confined to Wuhan, China, but they expanded to other Chinese cities [3] and then to other parts of the world. It can be observed from the demeanour of coronavirus that it was initially treated as an epidemic disease. However, as the cases of Coronavirus disseminate worldwide, it was upgraded to a pandemic disease. Initially, it was observed that the Coronavirus symptoms in human beings take 2 to 10 days to appear.

COVID-19 initially affected China and then the entire world, spreading to Europe, Germany, Italy, and America, and causing various deaths. Thousands of people have died as a result of COVID-19. COVID-19 also affected Asian countries, especially Malaysia. In Malaysia, the first case of the Coronavirus was reported on 25th January 2020 [4]. From 25th January 2020 to 14th May 2020, the statistics of cases show the escalation of Coronavirus rapidly. On the 14th of May 2020, WHO data revealed that there were 6779 total infected cases, 111 total reported fatalities, and 5351 total recovered patients [5].

As the spread of COVID-19 is very dangerous and has affected many people from various areas of the world, it is a crucial task for experts to calculate the gestures and transmission of Corona. Recently, many researchers investigated the reasons and transmission of Corona using different mathematical models [6]. Backer et al. [7] studied the incubation span of Corona among travellers from Wuhan, China. Rothe et al. [8] calculated the transmission of COVID-19 in Germany. Al-Tawfiq et al. [9] studied the effect of Coronavirus in the Middle East and calculated a case-control of COVID-19. Read et al. [10] investigated novel Coronavirus and estimated early epidemic parameters for the prediction of COVID-19. Jia et al. [11] studied the impact of the policy of interventions and also studied meteorological factors. Hellewell et al. [12] studied the control of COVID-19 by considering the case of isolation and contact. Imai et al. [I3] analysed the transmissibility of Corona. Chen et al. [14] investigated the similarity of COVID-19 and predicted the spread of Coronavirus.

Many researchers have reported different definitions of fractional parameters to investigate many physical phenomena. However, the dynamics and transmission of distinct infectious diseases, like the gesture of HIV investigated by [15], can be better described by the newly developed definition of the Atangana-Baleanu derivative. For example, chickenpox disease was studied by [16] using AB fractional derivative. Prakasha et al. [17] investigated hepatitis in their study. The mathematical model for the spread of dengue fever was developed by [18]. The AB time-fractional model for rubella disease was calculated by [19]. Sweilam et al. [20] investigated TB using the AB -fractional model and the effect of diabetes and resistant strains. AB time-fractional model applications are not limited to biological sciences, as they can be applied to various models of engineering. For example, Arif et al. [21] studied some engineering applications in CSF fluid flow using AB fractional model. Some nanofluid applications in couple stress fluid using the AB time-fractional model have been studied [22]. In another paper, Arif et al. [29, 30] discussed the comparison of various fractional operators with AB fractional operators and discussed some applications in the dynamics of the system.

The goal of this study is to use the SEIR model to explore the evolution and dissemination of corona in Malaysia. We also used the Atangana-Baleanu time-fractional model to transform the classical model. The AB time-fractional derivative was chosen because it has a non-local kernel and is non-singular, which could help anticipate corona spread in Malaysia more accurately. Additionally, we used corona data from May 1 to 14, 2020 to specify the supplied model to the real data in this study. The supplied model's positivity and invariance are also addressed in depth. The basic reproduction number and fixed points are anticipated. For the presented model, stability analysis and a few primitive properties have been proven. For the specified fractional dilemma, a numerical technique is built, and the results for the fractional parameter are graphed. For global asymptotical stability, a few graphs are displayed with varied initial conditions.

2. Mathematical Modelling

In this model, the spread of corona in humans has been discussed. Here $N_p(t)$ stands for the total population, which is divided into four sub-classes namely susceptible, exposed, infected, and recovered individuals represented by $S_p(t)$, $E_p(t)$, $I_p(t)$ and $R_p(t)$ respectively. The flow chart given below shows the interaction of these subclasses.

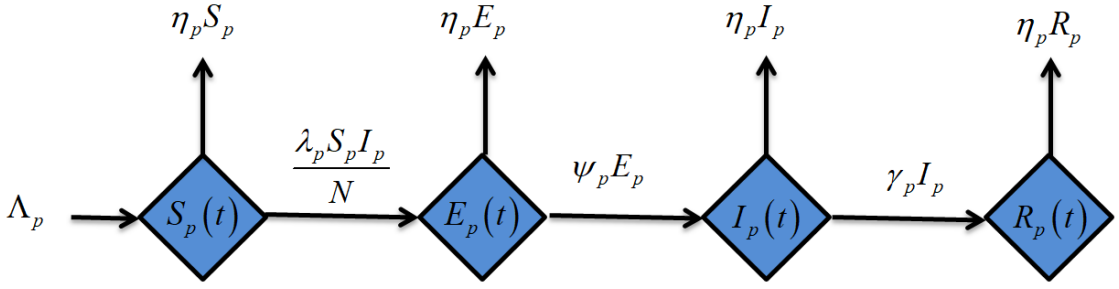

Figure 1: SEIR model Flow chart.

In this model, Λ_p is stand for the rate of recruitment of the susceptible population, which identify the birth rate, η_p represents each subclass death rate, λ_p shows the rate of interaction between infected and susceptible population with the transmit $\frac{\lambda_p S_p I_p}{N}$, the pace at which the exposed class finished their incubation time and joined the infected class is denoted by ψ_p, γ_p and is the recovery rate of the infected population.

$$\left.\begin{aligned} \frac{dS_p(t)}{dt} &= \Lambda_p - \eta_p S_p - \frac{\lambda_p S_p I_p}{N}, & \frac{dE_p(t)}{dt} &= \frac{\lambda_p S_p I_p}{N} - \eta_p E_p - \psi_p E_p, \\ \frac{dI_p(t)}{dt} &= \psi_p E_p - \eta_p I_p - \gamma_p I_p, & \frac{dR_p(t)}{dt} &= \gamma_p I_p - \eta_p R_p, \end{aligned}\right\}. \quad (1)$$

Corresponding initial conditions:

$$S(0) = S^* \geq 0\ ,\ E(0) = E^* \geq 0\ ,\ I(0) = I^* \geq 0 \text{ and } R(0) = R^* \geq 0. \quad (2)$$

3. Boundedness and Non-negativity of the Model

This section is included to demonstrate the boundedness and non-Negativity of the system's solutions (1). The following lemma is used to demonstrate the model's positivity.

Lemma 3.1. *Suppose* $\Phi \subset \mathbb{R} \times \mathbb{C}^n$ *is open,* $g_i \in \mathbb{C}(\Phi, \mathbb{R}), i = 1,2,3,...,n.$ *if* $g_i\big|_{x_i(t)=0, X_\tau \in \mathbb{C}^n_{+0}} \geq 0$, $X_t = (x_{1t}, x_{2t}, ..., x_{nt})^T, i = 1,2,...,n$ *then* $\mathbb{C}^n_{+0}\left\{\varphi = (\varphi_1, \varphi_2, ..., \varphi_n) : \varphi \in \mathbb{C}\left([-\upsilon, 0], \mathbb{R}^n_{+0}\right)\right\}$ *is the invariant domain of the below equations.*

$$\frac{dx_i(t)}{dt} = g_i\left(t, X_t\right), t \geq \sigma, i = 1,2,...,n. \tag{3}$$

Where,

$$\mathbb{R}^n_{+0}\left\{\left(x_1, x_2, ..., x_n\right) : x_i \geq 0, i = 1,2,...,n\right\}. \tag{4}$$

Preposition 3.1. *The system (1) is invariant in* $\mathbb{R}^4_+$

Proof: From system (1), we get:

$$\frac{dX}{dt} = M\left(X\left(t\right)\right), X(0) = X_0 \geq 0, \tag{5}$$

$$M\left(X(t)\right) = \left(M_1\left(X\right), M_2\left(X\right), M_3\left(X\right), M_4\left(X\right)\right)^T, \tag{6}$$

We noted that:

$$\left.\begin{aligned} &\left.\frac{dS_p(t)}{dt}\right|_{S_p=0} = \Lambda_p \geq 0, \qquad \left.\frac{dE_p(t)}{dt}\right|_{E_p=0} = \frac{\lambda_p S_p I_p}{S_p + I_p + R_p} \geq 0, \\ &\left.\frac{dI_p(t)}{dt}\right|_{I_p=0} = \psi_p E_p \geq 0, \qquad \left.\frac{dR_p(t)}{dt}\right|_{R_p=0} = \gamma_p I_p \geq 0 \end{aligned}\right\}. \tag{7}$$

In the light of Lemma 3.1, $\mathbb{R}^4_+$ is invariant set.

Preposition 3.2. *The system (1) is bounded in the region:*

$$\Phi = \left\{\left(S_p\left(t\right), E_p\left(t\right), I_p\left(t\right), R_p\left(t\right)\right) \in \mathbb{R}^4 : N_p(t) \leq \frac{\Lambda_p}{\eta_p}\right\}.$$

Proof: The sum of the equations mentioned in system (1), we can verified the Boundedness of the problem (1):

$$\frac{dN_p(t)}{dt} = \Lambda_p - \eta_p N_p, \text{ with } N_p(0) = N_0 \geq 0. \tag{8}$$

The solution of equation (8) becomes:

$$N_p\left(t\right) \leq N_0 e^{-\eta_p t} + \frac{\Lambda_p}{\eta_p}\left(1 - e^{-\eta_p t}\right). \tag{9}$$

From equation (9), we can observed that, if $t \to \infty$, $N_p(t) \leq \frac{\Lambda_p}{\eta_p}$ then , which specify the achievable area for the problem as follows:

$$\Phi = \left\{\left(S_p\left(t\right), E_p\left(t\right), I_p\left(t\right), R_p\left(t\right)\right) \in \mathbb{R}^4 : N_p(t) \leq \frac{\Lambda_p}{\eta_p}\right\}. \tag{10}$$

This solution shows the boundedness of the system (1).

4. Points of Equilibrium, Analysis of Local Stability and Basic Reproduction Number

This part comprises the model's possible fixed points (1). Disease Free Equilibrium (DFE) and Endemic Equilibrium (EE) are two alternative equilibrium points that can be determined (EE). Moreover, the next-generation technique calculates basic reproduction numbers and discusses the local stable analysis of these points of equilibrium. The model's steady-state solution is presented below, where the rate of change with function of time equals zero.

$$\left.\frac{dS_p(\tau)}{d\tau}=\frac{dE_p(\tau)}{d\tau}=\frac{dI_p(\tau)}{d\tau}=\frac{dR_p(\tau)}{d\tau}=0,\right\}. \tag{11}$$

Using equation (11), model (1) becomes:

$$\left.\begin{aligned}0&=\Lambda_p-\eta_pS_p-\frac{\lambda_pS_pI_p}{N},\\0&=\frac{\lambda_pS_pI_p}{N}-\eta_pE_p-\psi_pE_p,\\0&=\psi_pE_p-\eta_pI_p-\gamma_pI_p,\\0&=\gamma_pI_p-\eta_pR_p,\end{aligned}\right\}, \tag{12}$$

From the steady state system (12), DFE can be determined by letting $E_p=I_p=R_p=0$ and is considered by:

$$\Psi_{DFE}=\left(S^0,E^0,I^0,R^0\right)=\left(\frac{\Lambda_p}{\eta_p},0,0,0\right). \tag{13}$$

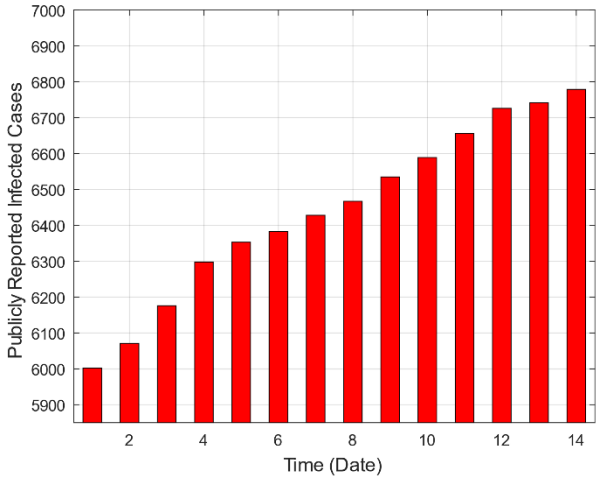

Figure 2. Two weeks (1st May 2020 to 14th May 2020) report of WHO for COVID-19 deaths.

Similarly, the model (1) of EE is determined from the system (12) and represented $\Psi_{EE}=\left(S^*,E^*,I^*,R^*\right)$. Where,

$$\left.\begin{aligned}S^*&=\frac{\Lambda_p\left(\eta_p^2-\gamma_p\psi_p-\eta_p\psi_p\right)}{\eta_p\left(\eta_p^2+\eta_p\gamma_p+\eta_p\lambda_p-\eta_p\psi_p-\lambda_p\psi_p\right)},\quad E^*=\frac{\Lambda_p\left(\eta_p\gamma_p+\eta_p\lambda_p+\gamma_p\psi_p-\lambda_p\psi_p\right)}{\left(\eta_p+\psi_p\right)\left(\eta_p^2+\eta_p\gamma_p+\eta_p\lambda_p-\eta_p\psi_p-\lambda_p\psi_p\right)},\\I^*&=\frac{\Lambda_p\left(\psi_p-\eta_p\right)\left(\eta_p\gamma_p+\eta_p\lambda_p+\gamma_p\psi_p-\lambda_p\psi_p\right)}{\gamma_p\left(\eta_p+\psi_p\right)\left(\eta_p^2+\eta_p\gamma_p+\eta_p\lambda_p-\eta_p\psi_p-\lambda_p\psi_p\right)},\quad R^*=\frac{\Lambda_p\left(\psi_p-\eta_p\right)\left(\eta_p\gamma_p+\eta_p\lambda_p+\gamma_p\psi_p-\lambda_p\psi_p\right)}{\eta_p\left(\eta_p+\psi_p\right)\left(\eta_p^2+\eta_p\gamma_p+\eta_p\lambda_p-\eta_p\psi_p-\lambda_p\psi_p\right)},\end{aligned}\right\}. \tag{14}$$

The basic reproduction number $\Re_0$ is determined by using the next-generation approach [23]. The matrices for F and V at (DFE) Ψ^0 are:

$$F=\begin{bmatrix}0&\lambda_p\\0&0\end{bmatrix}\text{ and }V=\begin{bmatrix}\eta_p+\psi_p&0_p\\\psi_p&\eta_p+\gamma_p\end{bmatrix}. \tag{15}$$

From reference [23], $\Re_0$ is equal to $\rho\left(FV^{-1}\right)$, where $\rho\left(FV^{-1}\right)$ is the spectral radius, which is determined as:

$$\Re_0 = \frac{\lambda_p \psi_p}{\left(\eta_p + \psi_p\right)\left(\eta_p + \gamma_p\right)}. \tag{16}$$

Theorem 4.1. *The DFE* Ψ^0 *of the system (1) is locally asymptotically stable if* $\Re_0 < 1$.

Proof: The Jacobian matrix under DFE of the system (1):

$$J_{\Psi^0} = \begin{bmatrix} -\eta_p & 0 & -\lambda_p & 0 \\ 0 & -\eta_p - \psi_p & \lambda & 0 \\ 0 & \psi_p & -\eta_p - \gamma_p & 0 \\ 0 & 0 & \gamma_p & -\eta_p \end{bmatrix}. \tag{17}$$

Suppose λ denotes the eigenvalues of the Jacobian matrix J_{Ψ^0}. Where, the two eigenvalues of the above-mentioned matrix are not positive, i.e. two time $-\eta_p$. The following characteristic equation can obtain the remaining required eigenvalues:

$$\lambda^2 + \kappa_1 \lambda + \kappa_2 = 0, \tag{18}$$

where,

$$\kappa_1 = \gamma_p + 2\eta_p + \psi_p, \tag{19}$$

$$\kappa_2 = \eta_p \gamma + \eta_p^2 + \gamma_p \psi_p - \lambda_p \psi_p$$
$$\Rightarrow \kappa_2 = \left(\eta_p + \gamma_p\right)\left(\eta_p + \psi_p\right)\left\{1 - \Re_0\right\}, \tag{20}$$

From equation (16), it can be noticed that $\kappa_1 > 0$. Similarly, from equation (17), it can be seen that $\kappa_2 > 0$ when $\Re_0 < 1$. Hence, the characteristics equation contain all the coefficients in non-negative form. Furthermore, the eigenvalues of the aforementioned characteristics equation are negative due to Rough-Hurtwiz criterion. Thus, all the eigenvalues of the Jacobian matrix (15) are negative for $\Re_0 < 1$. Accordingly the model mentioned in Eq. (1) is stable locally asymptotically when $\Re_0 < 1$.

5. Fractional Model and Numerical Scheme

5.1 Preliminaries

Definition: The Atangana-Baleanu fractional derivative is defined [24].

$${}^{AB}_{a}\boldsymbol{D}^{\alpha}_{\tau} f(t) = \frac{\Im(\alpha)}{1-\alpha}\int_a^{\tau} E_a\left(\frac{-\alpha\left(\tau - t\right)^{\alpha}}{1-\alpha}\right) f'\left(\tau\right) dt, \text{ for } \; 0 < \alpha < 1. \tag{21}$$

Here, $E_{\alpha}(.)$ represent Mittage-Leffler function and $\Im(\alpha)$ stand for normalization function [25].

Definition: For the determination of the fractional order ODE the numerical technique is mentioned in [26]: By

considering a non-linear fractional ODE:

$$ {}^{AB}\boldsymbol{D}_{\tau}^{\alpha} y(t) = f\left(t, y(t)\right) \ \text{ with } \ y(0) = y_0. \tag{22} $$

The numerical scheme for equation (22) is given by [Toufik and Atangana (2017)]:

$$ \begin{aligned} y_{n+1} &= y_0 + \frac{1-\alpha}{\mathfrak{I}(\alpha)} f\left(t_n, y(t_n)\right) \\ &+ \frac{\alpha}{\mathfrak{I}(\alpha)} \sum_{k=0}^{n} \left[\begin{array}{l} \dfrac{h^{\alpha} f\left(t_k, y(t_k)\right)}{\Gamma(\alpha+2)} \left\{ (n+1-k)^{\alpha} (n+2-k+\alpha) - (n-k)^{\alpha} (n+2-k+2\alpha) \right\} \\ -\dfrac{h^{\alpha} f\left(t_{k-1}, y(t_{k-1})\right)}{\Gamma(\alpha+2)} \left\{ (n+1-k)^{\alpha+1} - (n-k)^{\alpha} (n+1-k+\alpha) \right\} \end{array} \right]. \end{aligned} \tag{23} $$

5.2 Fractional Model

We substitute the classical time derivative with the AB time fractional derivative in order to generalize fractional model (1), and we get:

$$ \left. \begin{array}{ll} {}^{AB}_{0}\boldsymbol{D}_{t}^{\alpha} S_p(t) = \Lambda_p - \eta_p S_p - \dfrac{\lambda_p S_p I_p}{N}, & {}^{AB}_{0}\boldsymbol{D}_{t}^{\alpha} E_p(t) = \dfrac{\lambda_p S_p I_p}{N} - \eta_p E_p - \psi_p E_p, \\ {}^{AB}_{0}\boldsymbol{D}_{t}^{\alpha} I_p(t) = \psi_p E_p - \eta_p I_p - \gamma_p I_p, & {}^{AB}_{0}\boldsymbol{D}_{t}^{\alpha} R_p(t) = \gamma_p I_p - \eta_p R_p, \end{array} \right\}. \tag{24} $$

Here, α is the fractional parameter and ${}^{AB}_{0}\boldsymbol{D}_{t}^{\alpha}(.)$ is the AB time fractional derivative. These initial conditions and variables for the model (21) are positive.

5.3 Numerical Scheme

By applying the process mentioned in reference [26] on the model (21), we obtained the below form:

$$ \left. \begin{array}{ll} {}^{AB}_{0}\boldsymbol{D}_{t}^{\alpha} S_p(t) = \chi_1\left(t, S_p, E_p, I_p, R_p\right), & {}^{AB}_{0}\boldsymbol{D}_{t}^{\alpha} E_p(t) = \chi_2\left(t, S_p, E_p, I_p, R_p\right), \\ {}^{AB}_{0}\boldsymbol{D}_{t}^{\alpha} I_p(t) = \chi_3\left(t, S_p, E_p, I_p, R_p\right), & {}^{AB}_{0}\boldsymbol{D}_{t}^{\alpha} R_p(t) = \chi_4\left(t, S_p, E_p, I_p, R_p\right), \end{array} \right\}. \tag{25} $$

Furthermore, system (22) becomes:

$$ S_p(t) - S_p(0) = \frac{1-\alpha}{\mathfrak{I}(\alpha)} \chi_1\left(t, S_p, E_p, I_p, R_p\right) + \frac{\alpha}{\mathfrak{I}(\alpha)\Gamma(\alpha)} \int_0^t \chi_1\left(\zeta, S_p, E_p, I_p, R_p\right)(t-\zeta)^{\alpha-1} d\zeta, \tag{26} $$

$$ E_p(t) - E_p(0) = \frac{1-\alpha}{\mathfrak{I}(\alpha)} \chi_2\left(t, S_p, E_p, I_p, R_p\right) + \frac{\alpha}{\mathfrak{I}(\alpha)\Gamma(\alpha)} \int_0^t \chi_2\left(\zeta, S_p, E_p, I_p, R_p\right)(t-\zeta)^{\alpha-1} d\zeta, \tag{27} $$

$$ I_p(t) - I_p(0) = \frac{1-\alpha}{\mathfrak{I}(\alpha)} \chi_3\left(t, S_p, E_p, I_p, R_p\right) + \frac{\alpha}{\mathfrak{I}(\alpha)\Gamma(\alpha)} \int_0^{\tau} \chi_3\left(\zeta, S_p, E_p, I_p, R_p\right)(t-\zeta)^{\alpha-1} d\zeta, \tag{28} $$

$$ R_p(t) - R_p(0) = \frac{1-\alpha}{\mathfrak{I}(\alpha)} \chi_4\left(t, S_p, E_p, I_p, R_p\right) + \frac{\alpha}{\mathfrak{I}(\alpha)\Gamma(\alpha)} \int_0^{\tau} \chi_4\left(\zeta, S_p, E_p, I_p, R_p\right)(t-\zeta)^{\alpha-1} d\zeta. \tag{29} $$

By putting $t = t_{n+1}$, in equations 26-29 and using $n = 1, 2, \ldots$, we obtained:

$$S\left(t_{n+1}\right) - S\left(t_0\right) = \frac{1-\alpha}{\Im(\alpha)} \chi_1\left(t_n, S_p, E_p, I_p, R_p\right) + \frac{\alpha}{\Im(\alpha)\Gamma(\alpha)} \sum_{m=0}^{n} \int_{\tau_m}^{t_{m+1}} \chi_1\left(\zeta, S_p, E_p, I_p, R_p\right)\left(t_{n+1} - \zeta\right)^{\alpha-1} d\zeta, \tag{30}$$

$$E\left(t_{n+1}\right) - E\left(t_0\right) = \frac{1-\alpha}{\Im(\alpha)} \chi_2\left(t_n, S_p, E_p, I_p, R_p\right) + \frac{\alpha}{\Im(\alpha)\Gamma(\alpha)} \sum_{m=0}^{n} \int_{t_m}^{t_{m+1}} \chi_2\left(\zeta, S_p, E_p, I_p, R_p\right)\left(t_{n+1} - \zeta\right)^{\alpha-1} d\zeta, \tag{31}$$

$$I\left(t_{n+1}\right) - I\left(t_0\right) = \frac{1-\alpha}{\Im(\alpha)} \chi_3\left(t_n, S_p, E_p, I_p, R_p\right) + \frac{\alpha}{\Im(\alpha)\Gamma(\alpha)} \sum_{m=0}^{n} \int_{t_m}^{t_{m+1}} \chi_3\left(\zeta, S_p, E_p, I_p, R_p\right)\left(t_{n+1} - \zeta\right)^{\alpha-1} d\zeta, \tag{32}$$

$$R\left(t_{n+1}\right) - R\left(t_0\right) = \frac{1-\alpha}{\Im(\alpha)} \chi_4\left(t_n, S_p, E_p, I_p, R_p\right) + \frac{\alpha}{\Im(\alpha)\Gamma(\alpha)} \sum_{m=0}^{n} \int_{t_m}^{t_{m+1}} \chi_4\left(\zeta, S_p, E_p, I_p, R_p\right)\left(t_{n+1} - \zeta\right)^{\alpha-1} d\zeta. \tag{33}$$

Assuming the interval $\left[t_m, t_{m+1}\right]$ and applying the method of two-step Lagrange polynomial interpolation, equations (30)-(33) take place as under:

$$\begin{aligned} S\left(t_{n+1}\right) - S\left(t_0\right) &= \frac{1-\alpha}{\Im(\alpha)} \chi_1\left(t_n, S_p, E_p, I_p, R_p\right) \\ &+ \frac{\alpha}{\Im(\alpha)\Gamma(\alpha)} \sum_{m=0}^{n} \left(\frac{\chi_1\left(t_m, S_p, E_p, I_p, R_p\right)}{l} \int_{t_m}^{t_{m+1}} \left(\zeta - t_{m+1}\right)^{\alpha-1} \left(t_{n+1} - \zeta\right)^{\alpha-1} d\zeta \right) \\ &- \frac{\alpha}{\Im(\alpha)\Gamma(\alpha)} \sum_{m=0}^{n} \left(\frac{\chi_1\left(t_{m-1}, S_p, E_p, I_p, R_p\right)}{l} \int_{t_m}^{t_{m+1}} \left(\zeta - t_m\right)^{\alpha-1} \left(t_{n+1} - \zeta\right)^{\alpha-1} d\zeta \right), \end{aligned} \tag{34}$$

$$\begin{aligned} E\left(t_{n+1}\right) - E\left(t_0\right) &= \frac{1-\alpha}{\Im(\alpha)} \chi_2\left(t_n, S_p, E_p, I_p, R_p\right) \\ &+ \frac{\alpha}{\Im(\alpha)\Gamma(\alpha)} \sum_{m=0}^{n} \left(\frac{\chi_2\left(t_m, S_p, E_p, I_p, R_p\right)}{l} \int_{t_m}^{t_{m+1}} \left(\zeta - t_{m+1}\right)^{\alpha-1} \left(t_{n+1} - \zeta\right)^{\alpha-1} d\zeta \right) \\ &- \frac{\alpha}{\Im(\alpha)\Gamma(\alpha)} \sum_{m=0}^{n} \left(\frac{\chi_2\left(t_{m-1}, S_p, E_p, I_p, R_p\right)}{l} \int_{t_m}^{t_{m+1}} \left(\zeta - t_m\right)^{\alpha-1} \left(t_{n+1} - \zeta\right)^{\alpha-1} d\zeta \right), \end{aligned} \tag{35}$$

$$I\left(t_{n+1}\right)-I\left(t_0\right)=\frac{1-\alpha}{\Im(\alpha)}\chi_1\left(t_n,S_p,E_p,I_p,R_p\right)$$
$$+\frac{\alpha}{\Im(\alpha)\Gamma(\alpha)}\sum_{m=0}^{n}\left(\frac{\chi_3\left(t_m,S_p,E_p,I_p,R_p\right)}{l}\int_{t_m}^{t_{m+1}}\left(\zeta-t_{m+1}\right)^{\alpha-1}\left(t_{n+1}-\zeta\right)^{\alpha-1}d\zeta\right) \tag{36}$$
$$-\frac{\alpha}{\Im(\alpha)\Gamma(\alpha)}\sum_{m=0}^{n}\left(\frac{\chi_3\left(t_{m-1},S_p,E_p,I_p,R_p\right)}{l}\int_{t_m}^{t_{m+1}}\left(\zeta-t_m\right)^{\alpha-1}\left(t_{n+1}-\zeta\right)^{\alpha-1}d\zeta\right),$$

$$R\left(t_{n+1}\right)-R\left(t_0\right)=\frac{1-\alpha}{\Im(\alpha)}\chi_1\left(t_n,S_p,E_p,I_p,R_p\right)$$
$$+\frac{\alpha}{\Im(\alpha)\Gamma(\alpha)}\sum_{m=0}^{n}\left(\frac{\chi_4\left(t_m,S_p,E_p,I_p,R_p\right)}{l}\int_{\tau_m}^{t_{m+1}}\left(\zeta-t_{m+1}\right)^{\alpha-1}\left(t_{n+1}-\zeta\right)^{\alpha-1}d\zeta\right) \tag{37}$$
$$-\frac{\alpha}{\Im(\alpha)\Gamma(\alpha)}\sum_{m=0}^{n}\left(\frac{\chi_4\left(t_{m-1},S_p,E_p,I_p,R_p\right)}{l}\int_{t_m}^{t_{m+1}}\left(\zeta-t_m\right)^{\alpha-1}\left(t_{n+1}-\zeta\right)^{\alpha-1}d\zeta\right).$$

Where, the step size is l.

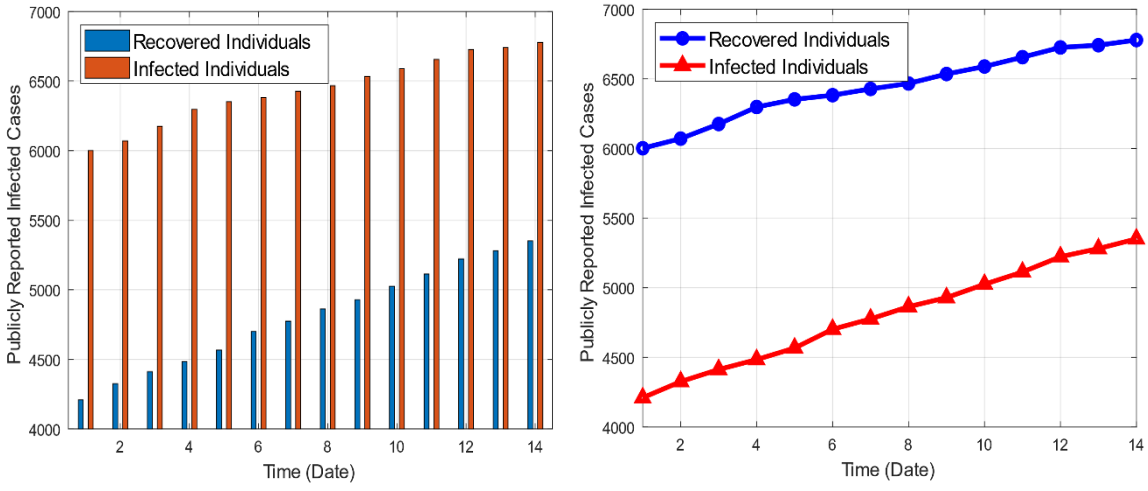

Figure 3. Comparison between disclosed deaths and recovered patients of COVID-19 in Malaysia and results are shown in the bar chart and line plot.

Equations (34)-(37) take on the following iterative structure when the integration terms in the aforementioned equations are solved:

$$S(t_{n+1}) = S(t_0) + \frac{1-\alpha}{\Im(\alpha)}\chi_1(t_n, S_p, E_p, I_p, R_p) + \frac{\alpha}{\Im(\alpha)}\sum_{m=0}^{n}\left[\begin{array}{l}\dfrac{l^\alpha \chi_1(t_m, S_p, E_p, I_p, R_p)}{\Gamma(\alpha+2)}\left\{(n+1-m)^\alpha(n+2-m+\alpha)-(n-m)^\alpha(n+2-m+2\alpha)\right\} \\ -\dfrac{l^\alpha \chi_1(t_{m-1}, S_p, E_p, I_p, R_p)}{\Gamma(\alpha+2)}\left\{(n+1-m)^{\alpha+1}-(n-m)^\alpha(n+1-m+\alpha)\right\}\end{array}\right], \tag{38}$$

$$E(t_{n+1}) = E(t_0) + \frac{1-\alpha}{\Im(\alpha)}\chi_2(t_n, S_p, E_p, I_p, R_p) + \frac{\alpha}{\Im(\alpha)}\sum_{m=0}^{n}\left[\begin{array}{l}\dfrac{l^\alpha \chi_2(t_m, S_p, E_p, I_p, R_p)}{\Gamma(\alpha+2)}\left\{(n+1-m)^\alpha(n+2-m+\alpha)-(n-m)^\alpha(n+2-m+2\alpha)\right\} \\ -\dfrac{l^\alpha \chi_2(t_{m-1}, S_p, E_p, I_p, R_p)}{\Gamma(\alpha+2)}\left\{(n+1-m)^{\alpha+1}-(n-m)^\alpha(n+1-m+\alpha)\right\}\end{array}\right], \tag{39}$$

$$I(t_{n+1}) = I(t_0) + \frac{1-\alpha}{\Im(\alpha)}\chi_3(t_n, S_p, E_p, I_p, R_p) + \frac{\alpha}{\Im(\alpha)}\sum_{m=0}^{n}\left[\begin{array}{l}\dfrac{l^\alpha \chi_3(t_m, S_p, E_p, I_p, R_p)}{\Gamma(\alpha+2)}\left\{(n+1-m)^\alpha(n+2-m+\alpha)-(n-m)^\alpha(n+2-m+2\alpha)\right\} \\ -\dfrac{l^\alpha \chi_3(t_{m-1}, S_p, E_p, I_p, R_p)}{\Gamma(\alpha+2)}\left\{(n+1-m)^{\alpha+1}-(n-m)^\alpha(n+1-m+\alpha)\right\}\end{array}\right], \tag{40}$$

$$R(t_{n+1}) = R(t_0) + \frac{1-\alpha}{\Im(\alpha)}\chi_4(t_n, S_p, E_p, I_p, R_p) + \frac{\alpha}{\Im(\alpha)}\sum_{m=0}^{n}\left[\begin{array}{l}\dfrac{l^\alpha \chi_4(t_m, S_p, E_p, I_p, R_p)}{\Gamma(\alpha+2)}\left\{(n+1-m)^\alpha(n+2-m+\alpha)-(n-m)^\alpha(n+2-m+2\alpha)\right\} \\ -\dfrac{l^\alpha \chi_4(t_{m-1}, S_p, E_p, I_p, R_p)}{\Gamma(\alpha+2)}\left\{(n+1-m)^{\alpha+1}-(n-m)^\alpha(n+1-m+\alpha)\right\}\end{array}\right]. \tag{41}$$

6. Data Fitting and Numerical Results

6.1 Data Fitting

We based our model solutions on real data received from WHO for Malaysia between May 1st and May 14th, 2020 [5]. Malaysia's total population for the year 2020 is 32,337,727 [27], according to stated data. We used $N(0) = 32337727$ for the initial values, with the exposed and infected persons being $E_p(0) = 10,000$ and $I_p(0) = 6819$ respectively. We

have combined the removed and recovered population in $R_p(t)$, so, $R_p(0)$ = dead+recovered $= 112 + 5439 = 5551$. The remaining population is treated as susceptible persons, so, $S_p(0) = 32315285$. For $\alpha = 1$, the mentioned model is fitted. The calculated reproduction number $\Re_0 \approx 1.79851$, for calculation we use different valves from table 1.

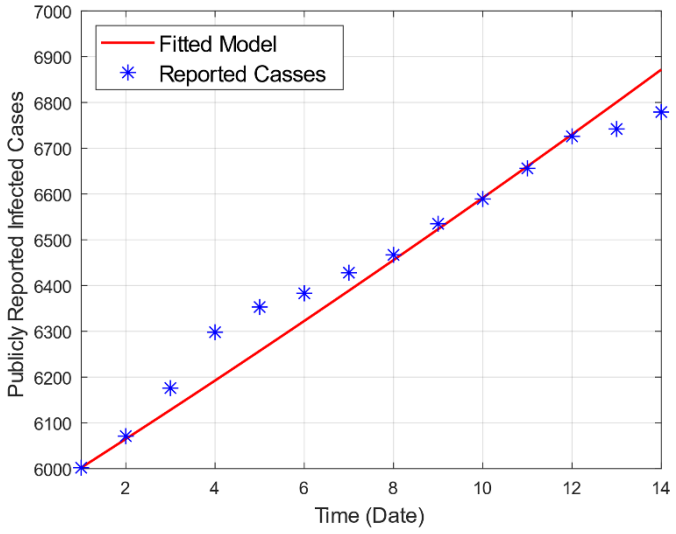

Figure 4. The comparison of real data versus model fitting data.

Parameter	Description	Value	Source
Λ_p	Birth rate	431,745.3538	Estimated
η_p	Natural Mortality rate	1/74.9 per 1000 people	[28]
λ_p	Contact rate	0.195	Fitted
ψ_p	Incubation period	0.145	Fitted
γ_p	Recovery rate	0.09744	Fitted

Table 1. Estimated and Fitted Values for Different Parameters of Model 1.

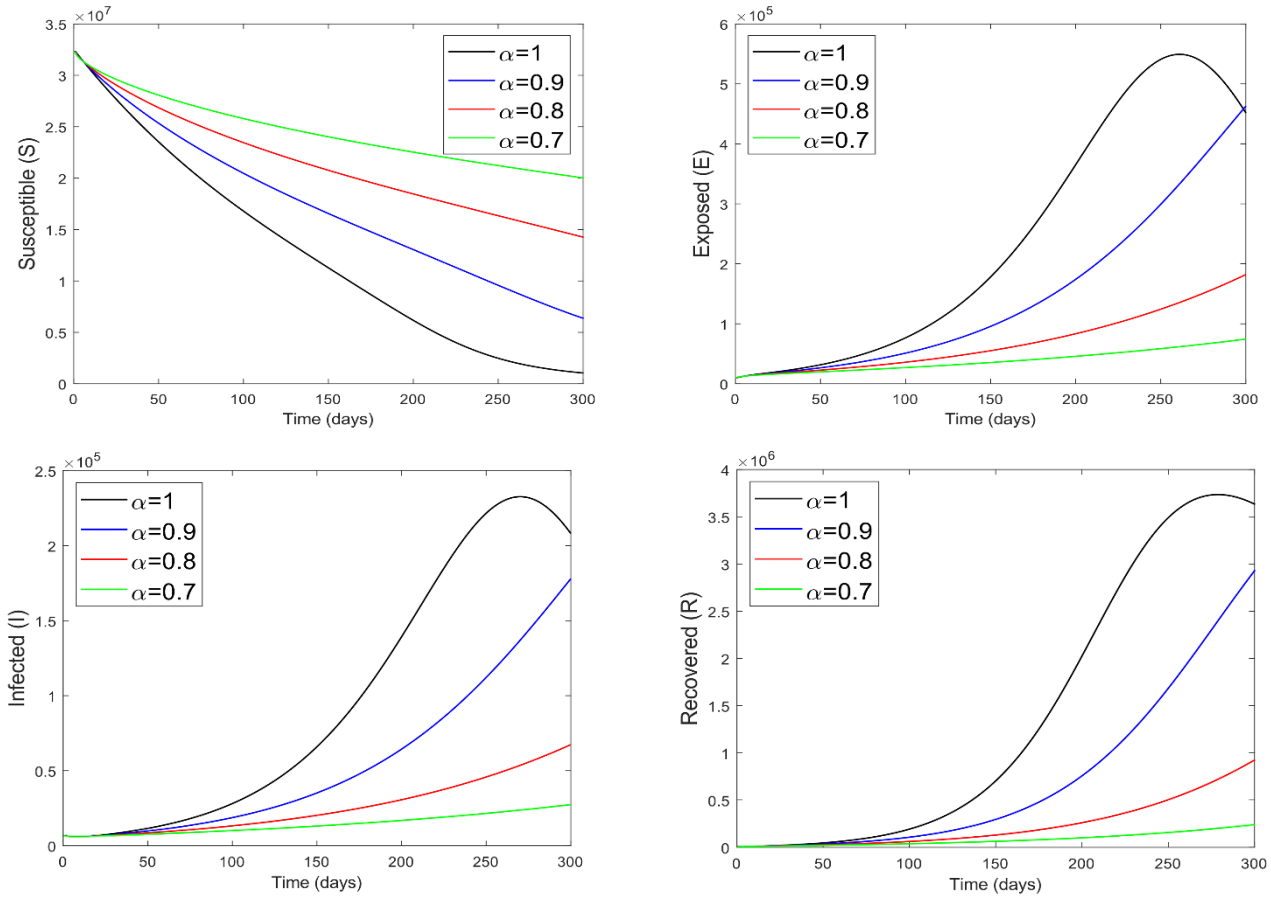

Figure 5. The passage and transmission of COVID-19 for various values of the fractional parameter α in different classes.

6.2 Numerical Results

The present section gives us graphical observations of the given model. Figure 1 represents the flow chart of the considered problem. To calculate the dynamics and transmission of COVIDS-19, we have considered the data collected by WHO from 1st May 2020 to 14th May 2020. In this interval, the spread of COVID-19 in Malaysia shows that the coronavirus spread at a high rate. Fig. 2 displays the number of deaths for COVID-19 in Malaysia using the time interval from 1st May 2020 to 14th May 2020. Fig. 3 highlights the comparative bar chart and line plot of described deaths and recovered persons of COVID-19 from 1st May 2020 to 14th May 2020. Fig. 4 depicts the comparison between the data of model and real data from WHO.

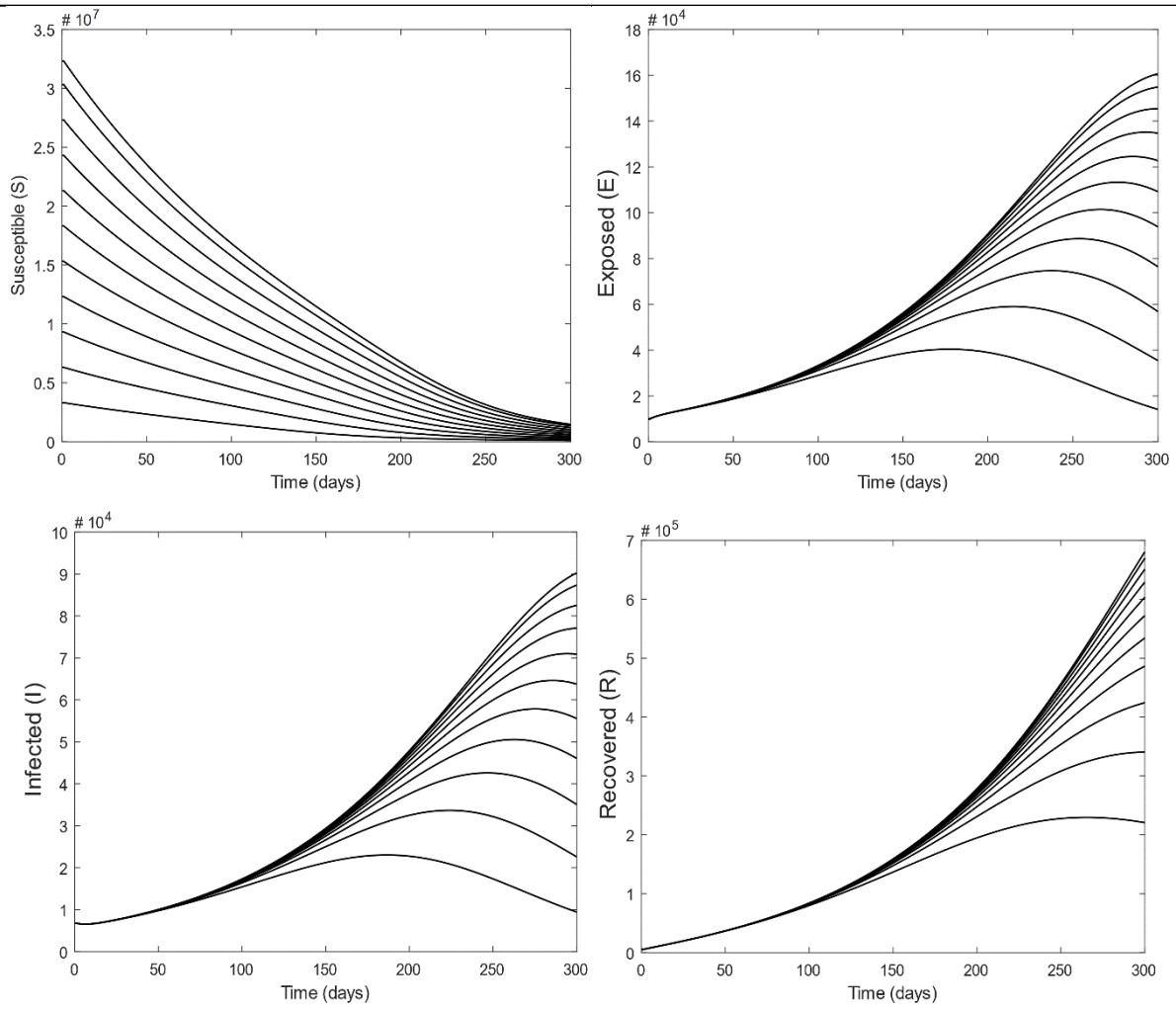

Figure 6. The gesture of COVID-19 in various initial conditions and classes.

To acquire findings from the provided model, we used MATLAB programme to replicate the given iterative approach. For the current COVID-19 model, the time unit is measured in days. The behaviour of various values of fractional parameters on the dynamic and transportation of COVID-19 for various subclasses of the total population is highlighted in Fig. 5. By varying α, various solutions of the given model are obtained. Furthermore, it can be seen from the graph that the gesture and transportation of COVID-19 have been predicted for the next 300 days. Finally, Fig. 6 is determined by taking the various initial values for endemic equilibrium's global asymptotical stability.

7. Concluding Remarks

For the behaviour and transmission of COVID-19, we used the SEIR model in this article. We have also established that the model in question is constrained and consistent. For the steady-state of the provided model, two equilibrium points, DFE and EE, are estimated. Moreover, $\Re_0$ is computed by applying the technique of next-generation. We found that the proposed model is locally asymptotically stable when $\Re_0 < 1$ using stability analysis. It means that by taking $\Re_0 < 1$ the disease from the population is dying out and the total population approaches to DFE.

We have also used the recently discovered AB fractional model to the classic SEIR model, which has been

generalised. The actual data have been fitted for the classical model i.e. $\alpha = 1$. We have chosen the value of $\Re_0 \approx 1.79851$, from the fitted values mentioned in table 1. For the results of the AB fractional model, a numerical approach is used. Various graphical results have been achieved after the computation of the numerical technique.

Moreover, we have forecasted the evolution and transmission of COVID-19 over the upcoming 300 days. The advantage of employing the AB fractional model lies in its capacity to yield multiple solutions. Through manipulation of the fractional parameter, researchers can align their empirical findings with our derived solutions, facilitating comparisons. Given that the management of infectious diseases remains a challenge both within Malaysia and globally, our findings offer insights. In the future, potential regulation strategies could involve integrating vaccination, quarantine, or a combination thereof into the existing model. This would enable us to showcase the influence of these interventions on the progression of this formidable infectious ailment.

Funding Statement: The author(s) received no specific funding for this study.

Conflicts of Interest: The authors declare that they have no interest in reporting regarding the present study.

REFERENCES

[1] P. K. Anderson, A. A. Cunningham, N. G. Patel, F. J. Morales, P. R. Epstein et al., "Emerging infectious diseases of plants: pathogen pollution, climate change and agrotechnology drivers," Trends in ecology & evolution, vol. 19, no. 10, pp. 535-544, 2004.

[2] D. Wang, B. Hu, C. Hu, F. Zhu, X. Liu et al., "Clinical characteristics of 138 hospitalized patients with 2019 novel coronavirus–infected pneumonia in wuhan, china," Jama, vol. 323, no. 11, pp. 1061-1069, 2020.

[3] Y. G. Sanchez, Z. Sabir and J. L. Guirao, "Design of a nonlinear SITR fractal model based on the dynamics of a novel coronavirus (COVID-19).

[4] S. A. Ñamendys-Silva, "Respiratory support for patients with COVID-19 infection," The Lancet Respiratory Medicine, vol. 8 no. 4, 2020.

[5] World Health Organization. (2020). Coronavirus disease 2019 (COVID-19): situation report, 88.

[6] J. T. Wu, K. Leung and G. M. Leung, "Nowcasting and forecasting the potential domestic and international spread of the 2019-ncov outbreak originating in wuhan, china: a modelling study," The Lancet, vol. 395, no. 10225, pp. 689-697, 2020.

[7] J. A. Backer, D. Klinkenberg and J. Wallinga, "Incubation period of 2019 novel coronavirus infections among travellers from wuhan, china, 20–28 January 2020," Eurosurveillance, vol. 25, no. 5, pp. 2000062, 2020.

[8] C. Rothe, M. Schunk, P. Sothmann, G. Bretzel, G. Froeschl et al., "Transmission of 2019-ncov infection from an asymptomatic contact in germany," New England Journal of Medicine, vol. 382, no. 10, pp. 970-971, 2020.

[9] J. A. Al-Tawfiq, K. Hinedi, J. Ghandour, H. Khairalla, S. Musleh et al., "Middle east respiratory syndrome coronavirus: a case-control study of hospitalized patients," Clinical Infectious Diseases, vol. 59, no. 2, pp. 160-165, 2014.

[10] J. M. Read, J. R. Bridgen, D. A. Cummings, A. Ho and C. P. Jewell, "Novel coronavirus 2019-ncov: early estimation of epidemiological parameters and epidemic predictions" MedRxiv, 2020.

[11] J. Jia, J. Ding, S. Liu, S. G. Liao, J. Li et al., "Modeling the control of covid-19: impact of policy interventions and meteorological factors," arXiv preprint arXiv:2003.02985, 2020.

[12] J. Hellewell, S. Abbott, A. Gimma, N. I. Bosse, C. I. Jarvis et al., "Feasibility of controlling COVID-19 outbreaks by isolation of cases and contacts," The Lancet Global Health, 2020.

[13] N. Imai, A. Cori, I. Dorigatti, M. Baguelin, C. A. Donnelly et al., "Report 3: transmissibility of 2019-ncov," Imperial College London. 2020.

[14] Z. Chen, W. Zhang, Y. Lu, C. Guo, Z. Guo et al., "From sars-cov to Wuhan 2019-ncov outbreak: similarity of early epidemic and prediction of future trends," Cell-Host-Microbe-D-20-00063, 2020.

[15] F. Evirgen, S. Uçar and N. Özdemir, "System analysis of HIV infection model with cd4+t under non-singular kernel derivative," Applied Mathematics and Nonlinear Sciences, vol. 5 no. 1, pp. 139-146, 2020.

[16] S. Qureshi and A. Yusuf, "Modeling chickenpox disease with fractional derivatives: from caputo to atangana-baleanu," Chaos, Solitons & Fractals, vol. 122, pp. 111-118, 2019.

[17] D. G. Prakasha, P. Veeresha and H. M. Baskonus, "Analysis of the dynamics of hepatitis-E virus using the atangana-baleanu fractional derivative," The European Physical Journal Plus, vol. 134, no. 5, pp. 241, 2019.

[18] S. Qureshi and A. Atangana, "Mathematical analysis of dengue fever outbreak by novel fractional operators with field data," Physica A: Statistical Mechanics and its Applications, vol. 526, pp. 121-127, 2019.

[19] I. Koca, "Analysis of rubella disease model with non-local and non-singular fractional derivatives," An International Journal of Optimization and Control: Theories & Applications (IJOCTA), vol. 8 no. 1, pp. 17-25, 2017.

[20] N. H. Sweilam, S. M. Al-Mekhlafi and D. Baleanu, "Optimal control for a fractional tuberculosis infection model including the impact of diabetes and resistant strains," Journal of Advanced Research, vol. 17, pp. 125-137, 2019.

[21] M. Arif, F. Ali, N. A. Sheikh, I. Khan and K. S. Nisar, "Fractional model of couple stress fluid for generalized couette flow: a comparative analysis of atangana–baleanu and caputo–fabrizio fractional derivatives," IEEE Access, vol. 7, pp. 88643-88655, 2019.

[22] M. Arif, F. Ali, I. Khan and K. S. Nisar, "A time fractional model with non-singular kernel the generalized couette flow of couple stress nanofluid," IEEE Access, vol. 8, pp. 77378-77395, 2020.

[23] P. Van den Driessche and J. Watmough, "Reproduction numbers and sub-threshold endemic equilibria for compartmental models of disease transmission," Mathematical Biosciences, vol. 180, no. 1 and 2, 29-48, 2002.

[24] Atangana, A., & Baleanu, D., "New fractional derivatives with nonlocal and non-singular kernel: theory and application to heat transfer model", arXiv preprint arXiv:1602.03408, 2016.

[25] N. Sene, "SIR epidemic model with mittag–leffler fractional derivative," Chaos, Solitons & Fractals, vol. 137, pp. 109833, 2020.

[26] M. Toufik and A. Atangana, "New numerical approximation of fractional derivative with non-local and non-singular kernel: application to chaotic models," The European Physical Journal Plus, vol. 132 no. 10, pp. 444, 2017.

[27] Population of Malaysia 2020. https://www.worldometers.info/world-population/malaysia-population/.

[28] Natural mortality rate of Malaysia, https://en.wikipedia.org/wiki/Healthcare_in_Malaysia.

[29] Arif, M., Kumam, P., Kumam, W., Riaz, M. B., & Khan, D. (2022). A comparative analysis of multiple fractional solutions of generalized Couette flow of couple stress fluid in a channel. Heat Transfer, 51(8), 7348-7368.

[30] Arif, M., Kumam, P., Kumam, W., & Mostafa, Z. (2022). Heat transfer analysis of radiator using different shaped nanoparticles water-based ternary hybrid nanofluid with applications: A fractional model. Case Studies in Thermal Engineering, 31, 101837.